CONF-770607--4

A PULSED POWER SUPPLY FOR INJECTION BUMP MAGNETS

W. F. Praeg

Prepared for

IEEE
1977 Power Electronics Specialists
San Francisco, California
June 14-16, 1977

U of C-AUA-USERDA

ARGONNE NATIONAL LABORATORY, ARGONNE, ILLINOIS

operated under contract W-31-109-Eng-38 for the
U. S. ENERGY RESEARCH AND DEVELOPMENT ADMINISTRATION

A PULSED POWER SUPPLY FOR INJECTION BUMP MAGNETS*

W. F. Praeg
Argonne National Laboratory
Argonne, Illinois

Summary

A very precise and relatively inexpensive charging circuit for an energy storage capacitor bank feeds an efficient thyristor-controlled pulse-forming discharge circuit. These circuits, which generate magnet pulses of 300 joules at a rate of 30 per second, are analyzed in this paper.

Introduction

For injection of H^- ions at 50 MeV into a synchrotron at Argonne National Laboratory, three injection bump magnets must be pulsed 30 times per second. Figure 1 shows the orbit deformation produced by the magnets during injection.

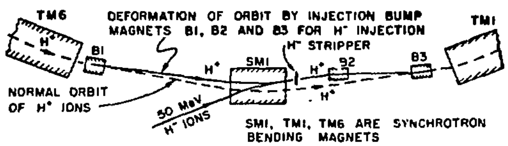

Fig. 1. H^- injection at 50 MeV into a 500 MeV synchrotron.

Figure 2 shows the desired current pulse and associated magnet voltage for the series-connected magnets. The current rises sinusoidally to its peak value of 3 kA in 500 μs. After the current has passed its peak, it decays exponentially during the beam-injection time. At the end of injection, the current must be turned off within 125 μs because the magnetic field would interfere with beam acceleration. The current shape during turnoff is unimportant and, for this reason, is shown as a straight line in Fig. 2. Different modes of injection require that the time constant of the injection field be adjustable between 1.2 ms (solid waveforms in Fig. 2) and 0.45 ms (dotted waveforms in Fig. 2). No commutation spikes may appear in the current waveform.

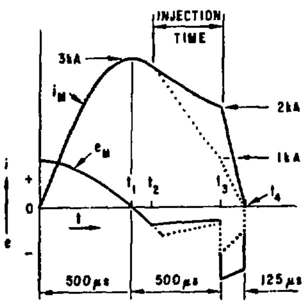

Fig. 2. Desired current and voltage for beam bump magnets.

*Work supported by the U. S. Energy Research and Development Administration.

A Pulsed Power Supply With Limited Energy Recovery

Figure 3 is a schematic diagram of a charging circuit to store energy in capacitor C_1 and of a discharge circuit which generates the desired magnet pulse with a minimum number of circuit components.

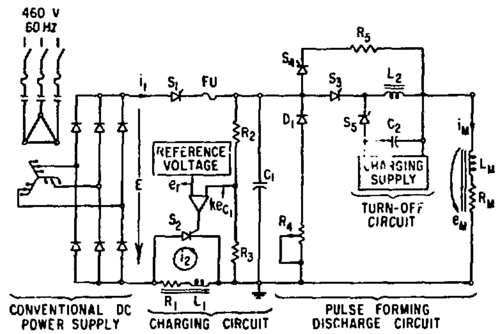

Fig. 3. Power supply for beam bump magnets.

A Controlled Charging-Choke Circuit with Energy Recovery

When thyristor S_1 is turned on, the unregulated voltage E of a conventional dc power supply is applied to a charging circuit comprising L_1, C_1, and R_1. As shown in Fig. 4, voltage E drives a sinusoidal current i_1. Between times t_1 and t_2, the decaying current generates a voltage $L_1\, di_1/dt$, which aids the supply voltage E to charge capacitor C_1 to a voltage greater than E. When $R_1 \to 0$, this voltage would be, at time t_2, $e_{C_1} = 2E$.

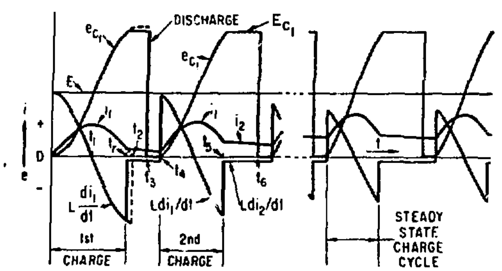

Fig. 4. Currents and Voltages of the Charging Circuit of Figure 3.

With thyristor S_2 across the charging choke L_1, we can terminate the charging cycle at any instant between times t_1 and t_2. The charging circuit compares a fraction of the capacitor voltage ke_{C_1} with a reference voltage e_r. At time t_r, when these voltages are equal, a pulse is generated which turns S_2 on.

With S_2 conducting, the driving voltage $L_1\, di_1/dt$ is removed from the circuit, and with the capacitor voltage e_{C_1} larger than the power-supply voltage E, thyristor S_1 is back biased and turns off, thereby stopping the charging current i_1. Thus capacitor C_1 is charged to a very precisely controlled voltage E_{C_1} (error ± 0.1%) from a poorly regulated (± 2%) dc power supply.

The current i_2 flowing in choke L_1 at time t_r will decay with a time constant of $\sim L_1/R_1$. At time t_3, capacitor C_1 discharges into the magnet load. Thyristor S_2 remains turned on by the circulating current i_2 until time t_4, when the next charging cycle is initiated by turning on S_1.

With S_1 conducting, the supply voltage E is back-biasing S_2 and thereby turning it off. This returns the choke to the charging circuit, and the above cycle repeats. The current i_2 flowing in the choke when S_2 is turned off will aid in charging capacitor C_1. The energy $0.5\, L_1\, i_2^2$ is returned to the circuit. This makes the charging circuit not only a very precise voltage regulator, but also very efficient.

The range of the capacitor voltage $E_{C_1} = e_r/k$ is controlled by selecting the appropriate taps on the rectifier transformer for a choice of supply voltage E. By adjusting the reference voltage e_r, we can obtain any voltage value E_{C_1} within a given range. Table 1 shows the three overlapping ranges that cover voltages E_{C_1} from 200 to 800 V.

Table 1. Ranges of Capacitor Voltage E_{C_1}

Power Supply Voltage E	Range of E_{C_1} Controlled by Setting of e_r
Tap 1: 187 V	200-365 V
Tap 2: 271 V	290-529 V
Tap 3: 410 V	439-800 V

As shown in Fig. 4, it takes several charging cycles with increasing peak currents to reach the steady-state waveform. When S_1 is turned on, the charging current i_1 and the capacitor voltage e_{C_1} follow the equations

$$i_1 = I_o \varepsilon^{-\alpha t} \cos \omega t + \frac{E - I\, R_1/2}{\omega L_1} \varepsilon^{-\alpha t} \sin \omega t, \qquad (1)$$

and

$$e_{C_1} = I_c L_1 \left[\alpha - \varepsilon^{-\alpha t} (\alpha \cos \omega t - \omega \sin \omega t) \right] +$$

$$+ (E - I_o R_1/2) \left[1 - \varepsilon^{-\alpha t} \left(\frac{\alpha}{\omega} \sin \omega t + \cos \omega t\right) \right], \qquad (2)$$

where

I_o = current circulating in L_1 at t_o,

$\alpha = R_1/2L_1$,

$\omega = (1/L_1C_1 - \alpha^2)^{1/2}$,

and

E = Power-supply voltage.

The waveshapes illustrated in Fig. 4 are shown in detail in Fig. 5 for a desired capacitor voltage of $E_{C_1} = 800$ V. The first charge cycle takes $t_r = 23.1$ ms and ends at time t_r with a choke current of $i_{2_{t_r}} = 15.2$ A. The current then circulates through L_1 for 10.2 ms, during which time it decays to

$$i_{2_{t_4}} = i_{2_{t_r}} \varepsilon^{-\frac{R_1}{L_1}(t_4 - t_r)} = 15.2 \text{ A } \varepsilon^{-\frac{0.1}{0.038} 0.0102} = 14.8 \text{ A}. \qquad (3)$$

The second charge cycle begins at t_4 with $i_2 = 14.8$ A and lasts for 21 ms, ending at time t_5 with a current of $i_{2_{t_5}} = 22$ A. After a few more cycles, a steady-state condition is reached with current and voltage waveforms as shown in Fig. 5.

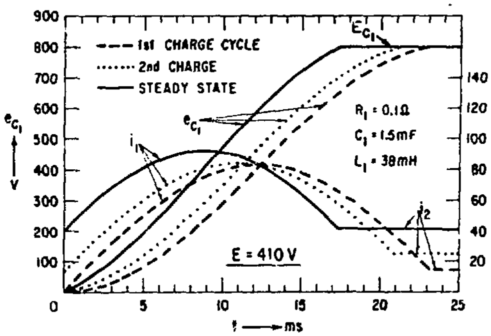

Fig. 5. Currents and voltages of the charging circuit of Figure 3 for E = 410 V.

A Discharge Circuit Without Energy Recovery.

With C_1 charged to E_{C_1}, a magnet pulse as illustrated in Fig. 6 is initiated with the circuit of Fig. 3 by turning on thyristor S_3. Capacitor voltage E_{C_1} drives a sinusoidally rising current of

$$i_M = \frac{E_{C_1}}{\omega_1 L} \varepsilon^{-\alpha_1 t} \sin \omega_1 t, \qquad (4)$$

where

$L = L_M + L_2 = 60\ \mu H + 7\ \mu H = 67\ \mu H$,

$\alpha_1 = R/2L$,

$\omega_1 = (1/LC_1 - \alpha_1^2)^{1/2}$,

and

R = total effective circuit resistance.

The current reaches its peak at time

$$t_1 = \frac{1}{\omega_1} \tan^{-1} \frac{\omega_1}{\alpha_1}. \qquad (5)$$

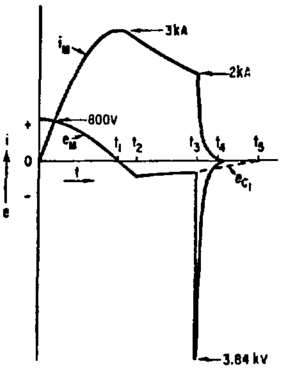

Fig. 6.

Magnet pulse generated by the discharge circuit of Figure 3.

After the current has reached its peak, the voltage on C_1 reverses its polarity and the current begins to transfer into the crowbar consisting of adjustable resistor R_4 and diode D_1; D_1 was back-biased by e_{C_1} during the current rise. This current transfer takes place between times t_1 and t_2. For oscillatory circuit conditions, the current and voltage shapes during transfer are

$$i_{C_1} = i_{t_1} \varepsilon^{-\alpha_2 t} \left(\cos \omega_2 t - \frac{\alpha_2}{\omega_2} \sin \omega_2 t\right) , \quad (6)$$

$$e_{C_1} = \frac{i_{t_1}}{C_1} \frac{\alpha_2}{\alpha_2^2+\omega_2^2} \left\{\left[1-\varepsilon^{-\alpha_2 t} \left(\cos \omega_2 t - \frac{\omega_2}{\alpha_2} \sin \omega_2 t\right)\right] - \left[1-\varepsilon^{-\alpha_2 t}\left(\frac{\alpha_2}{\omega_2} \sin \omega_2 t + \cos \omega_2 t\right)\right]\right\} , \quad (7)$$

$$i_{R_4} = \frac{i_{t_1}}{\omega_2 C_1 R_4} \varepsilon^{-\alpha_2 t} \sin \omega_2 t , \quad (8)$$

and

$$e_{R_4} = e_{C_1} = \frac{i_{t_1}}{\omega_2 C_1} \varepsilon^{-\alpha_2 t} \sin \omega_2 t , \quad (9)$$

where

$$\alpha_2 = \frac{R_4 R_M C_1 + L}{2 L C_1 R_4} ,$$

$$\omega_2 = \left(\frac{R_4+R_M}{L C_1 R_4} - \alpha_2^2\right)^{1/2} ,$$

$$L = L_M + L_2 ,$$

and

$$t = \text{time after } t_1 \text{ in Fig. 6.}$$

If the crowbar resistor overdamps the circuit, $\alpha_2^2 > (R_4+R_M)/LC_1R_4$, the above equations change to

$$i_{C_1} = i_{t_1} \varepsilon^{-\alpha_3 t} \left(\cosh \omega_3 t - \frac{\alpha_3}{\omega_3} \sinh \omega_3 t\right) , \quad (10)$$

$$e_{C_1} = \frac{i_{t_1}}{C_1} \frac{\alpha_2}{\alpha_2^2-\omega_3^2} \left\{\left[1-\varepsilon^{-\alpha_2 t} \left(\cosh \omega_3 t + \frac{\omega_3}{\alpha_2} \sinh \omega_3 t\right)\right] - \left[1-\varepsilon^{-\alpha_2 t}\left(\frac{\alpha_2}{\omega_3} \sinh \omega_3 t + \cosh \omega_3 t\right)\right]\right\} , \quad (11)$$

$$i_{R_4} = \frac{i_{t_1}}{\omega_3 R_4 C_1} \varepsilon^{-\alpha_2 t} \sinh \omega_3 t , \quad (12)$$

and

$$e_{R_4} = \frac{i_{t_1}}{\omega_3 C_1} \varepsilon^{-\alpha_2 t} \sinh \omega_3 t , \quad (13)$$

where

$$\omega_3 = \left(\alpha_2^2 - \frac{R_4+R_M}{L C_1 R_4}\right)^{1/2} .$$

At time t_2, the current transfer is completed. Figure 7 shows voltage and current shapes during the transfer time for various values of R_4.

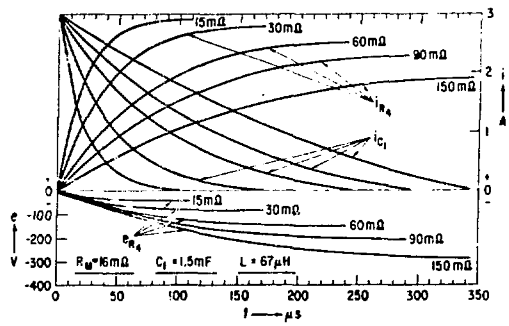

Fig. 7. Currents and voltages during transfer of current into crowbar.

Between times t_2 and t_3, the exponentially decaying magnet current and voltage shown in Fig. 6 are given by

$$i_M = i_{t_2} \varepsilon^{-\frac{R_4+R_M}{L_2+L_M} t} , \quad (14)$$

and

$$\hat{e}_M = \left[R_M - \frac{L_M(R_4+R_M)}{L_2+L_M}\right] i_{t_2}\, \varepsilon^{-\frac{R_4+R_M}{L_2+L_M}t} \quad . \qquad (15)$$

Injection is terminated at time t_3 when thyristors S_4 and S_5 are turned on. This causes the charge on capacitor C_2 to discharge through L_2 via S_5 and through R_5 via S_5, S_3, and S_4. The reverse current through S_3 and the reverse voltage provided by the voltage on C_2 will turn off S_3 in ≤ 25 μs. Thyristor S_5 turns off when the current in the oscillatory L_2C_2 circuit tries to reverse after C_2 has reached its negative peak voltage. Figure 8 illustrates current and voltage waveforms of the turnoff circuit.

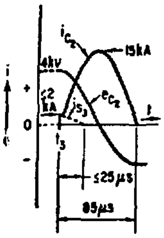

Fig. 8. Discharge of turnoff circuit of Figure 3.

When S_3 turns off, the magnet discharges into $R_M+R_4+R_5$. As shown in Fig. 6, the magnet coil is then exposed to a peak voltage of

$$\hat{e}_M = L_M \frac{di_{t_3}}{dt} - i_{t_3} R_M = i_{t_3} (R_4+R_5) \quad . \qquad (16)$$

At the end of the 125 μs turnoff time, at time t_4, we can tolerate a current that is $\leq 2\%$ of the current flowing at time t_3. This requires a time constant for the turnoff circuit of $\tau \leq L_M/(R_M+R_4+R_5) \leq 125$ μs$/4 \leq 31.25$ μs. With $L_M = 60$ μH, we require $R_M+R_4+R_5 \geq 60/31.25 \geq 1.92$ Ω; almost all of this resistance value is provided by R_5. This forces a peak magnet driving voltage of $\hat{e}_M \approx 1.92$ Ω × 2 kA = 3.84 kV. The negative charge on C_1 is dissipated in R_4 between times t_3 and t_5.

The relatively simple discharge circuit shown in Fig. 3 has the following very undesirable features:

(a) The magnet voltage at turnoff is ∿ 3.8 kV.

(b) The coil windings of the magnets and of inductor L_2 must be rated for 4 kV.

(c) Thyristor assemblies S_3, S_4, and S_5 must be rated for 4 kV.

(d) The 105 μF turnoff capacitor C_2 must be rated for 4 kV.

(e) The turnoff circuit carries a peak current of 15 kA.

(f) The energies stored at the end of injection in the magnets and in C_1 are lost. These energies, at 2 kA and R_4 = 50 mΩ, will amount to 120 J in the magnet and 7.5 J in C_1. They cause losses of 3.83 kW at a 30 Hz repetition rate.

(g) A 4 kV charging power supply is required for the turnoff circuit.

A Pulsed Power Supply With Optimum Energy Recovery

To avoid the shortcomings of the circuit of Fig. 3, we developed the more sophisticated circuit shown in Fig. 9. A typical magnet pulse generated by this circuit is shown in Fig. 10.

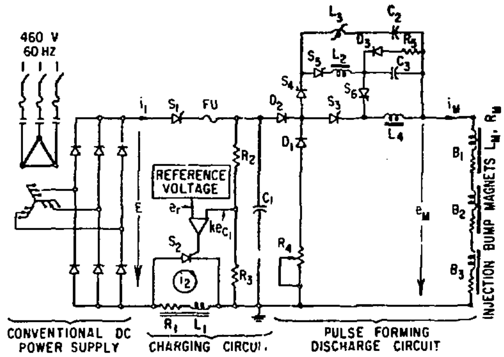

Fig. 9. Power supply with optimized energy recovery.

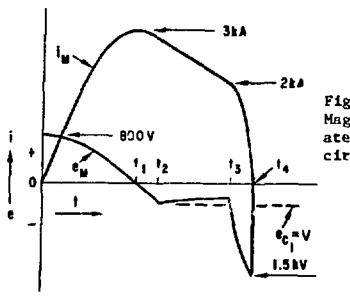

Fig 10. Magnet pulse generated by the discharge circuit of Figure 9.

Controlled Charging-Choke Circuit with Energy Recovered from C_1.

A negative charge is accumulated on C_1 when the magnet is crowbarred by diode D_1 with resistor R_4 at time t_2 in Fig. 10. Diode D_2 prevents this charge from dissipating in R_4. This is shown as a dashed line e_{C_1} = V in Fig. 10 and has a profound effect on circuit efficiency. The energies stored in C_1 and in L_1 at the end of a magnet pulse will aid the dc power supply in charging C_1 to E_{C_1} for the next magnet pulse.

As shown in Fig. 11, the very first charging pulse of the circuit of Fig. 9 is identical to the first one of the circuit of Fig. 3. However, in the circuit of Fig. 9, the negative charge on C_1, proportional to the trapped voltage V, will cause all subsequent charging pulses to have an energy boost proportional to V^2. This causes the charge time of subsequent pulses to decrease and the circulating current i_2 in the charging choke to increase. This process continues until a steady-state condition is reached.

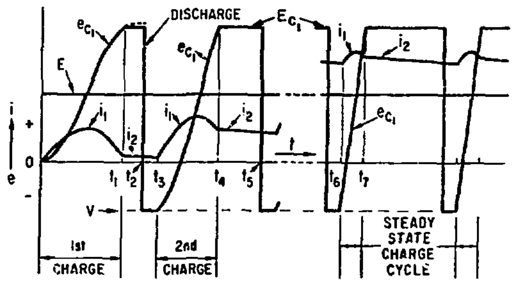

Fig. 11. Currents and voltages of the charging circuit of Figure 9.

For the circuit of Fig. 9, the charging current i_1 and voltage e_{C_1} can be written

$$i_1 = I_0\varepsilon^{-\alpha t}\cos \omega t + \frac{E+V-I_0R_1/2}{\omega L_1}\varepsilon^{-\alpha t}\sin \omega t \quad (1')$$

and

$$e_{C_1} = I_0L_1\left[\alpha - \varepsilon^{-\alpha t}(\alpha \cos \omega t - \omega \sin \omega t)\right] +$$

$$+ (E+V-I_0R_1/2\left[1-\varepsilon^{-\alpha t}\left(\frac{\alpha}{\omega}\sin \omega t + \cos \omega t\right)\right], \quad (2')$$

where

V = negative voltage on C_1 at t_0.

As illustrated in Fig. 12, with a power-supply voltage of $E = 410$ V, the time for the initial charge to reach 800 V from zero is 23.1 ms, ending with a circulating current of 15.2 A. All subsequent pulses begin with $V = -280$ V on capacitor C_1. The second charge has a duration of only ∿17 ms and ends with a circulating current of ∿110 A. Finally, a stable condition is reached with a charge time of ∿6 ms and a circulating current of ∿270 A. This high circulating current causes i^2R losses of about 6.5 kW in the charging choke L_1.

Figure 13 is an oscilloscope picture of successive traces of capacitor voltage e_{C_1}. In this example, the time for the very first charge, starting from zero voltage, is 18 ms. It takes about six more charge cycles of ever-decreasing duration to reach a steady-state charge time of about 5 ms.

The operating conditions illustrated by Figs. 11-13 result in high losses in the charging-choke coil and therefore compare poorly with the ones shown in Fig. 5. for the circuit of Fig. 3. However, they can easily be corrected by operating the more efficient circuit of Fig. 9 from a lower supply voltage. Tapping the rectifier transformer back to a dc output voltage of $E = 271$ V provides a steady-state capacitor voltage of 800 V with a charge pulse of 19 ms duration and a circulating current of $i_2 = 41.2$ A, as shown in Fig. 14. Recovering the negative charge on capacitor C_1 has reduced the power drawn from the line.

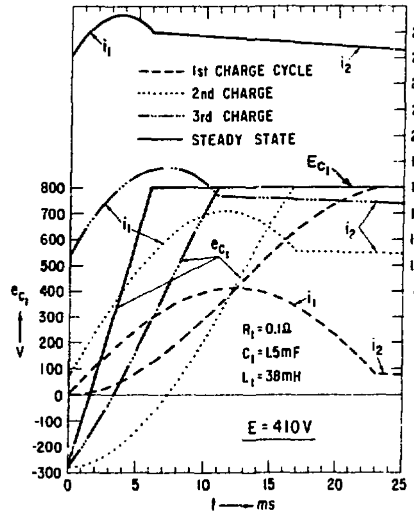

Fig. 12. Currents and voltages of the charging circuit of Figure 9 for $E = 410$ V and $E_{C_1} = 800$ V.

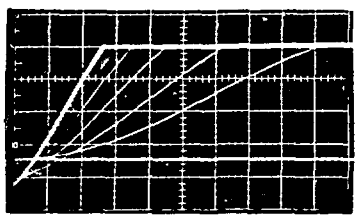

200 V/cm

→ 2 ms/cm

Fig. 13. Oscilloscope picture of capacitor voltage e_{C_1} during initial charging pulses.

<u>Startup of Charging-Choke Circuit</u>. In the circuit of Fig. 3, the peak voltage on capacitor C_1 is always less than twice the supply voltage; that is, $E_{C_1} < 2E$. To start operation, the reference voltage is set for the desired operating voltage $e_r = kE_{C_1}$ and the circuit will then perform as shown in Figs. 4 and 5. To operate the charging-choke circuit of Fig. 9 economically, the desired capacitor voltage must be larger than twice the supply voltage, that is $E_{C_1} > 2E$, as illustrated by the steady-state condition shown in Fig. 14. With this circuit, steady-state charging conditions can be reached in two different ways.

a. The reference voltage e_r is set for the desired operating voltage $e_r = kE_{C_1}$. Since $E_{C_1} > 2E$, the first charging pulse will not reach E_{C_1}. As a consequence, thyristor S_2 will not be turned on and the circuit operates during the first charge like an ordinary charging-choke circuit. For example, with $E = 271$ V and $E_{C1} = 800$ V, capacitor C_1 will be initially charged to $e_{C1} \leq 542$ V. When the capacitor discharges, this voltage will drive a peak current of only 2 kA through the magnets. During the first discharge, a voltage of $V = -190$ V is trapped on C_1. This voltage will aid in the second cycle to charge C_1 to a higher voltage. In this way, the circuit reaches steady state after a few pulses.

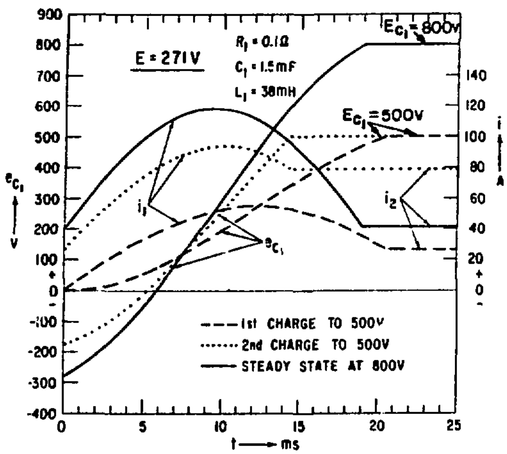

Fig. 14. Currents and voltages of the charging circuit of Figure 9 for $E = 271$ V and $E_{C1} =$ 500 and 800 V.

b. Another, perhaps less convenient, way of startup is as follows. The reference voltage is initially set for $e_r/k < 2E$. After the first pulse, energy will be stored in both C_1 and L_1. The reference voltage can now be increased to the desired operating conditions. For example, with $E = 271$ V and $E_{C1} = 800$ V, one could initially set $e_r/k = 500$ V. As shown in Fig. 14, after the first pulse of 20.5 ms duration, we have a circulating current of $i_2 = 26$ A in L_1, and a voltage of $V = -175$ V on C_1. These energies shorten the second pulse to 14.5 ms and leave $V = -175$ V and $i_2 = 79$ A stored. The reference voltage can now be increased to the desired value of $e_r/k = E_{C1} = 800$ V. Stable operation will be obtained within a few pulses with a charge time of 19 ms and $i_2 = 41.2$ A.

Discharge Circuit with Energy Recovery.

When the magnets are to be pulsed for the first time, the only component of the discharge circuit of Fig. 9 with stored energy is capacitor C_1. Therefore, the sequence of the operation is as follows:

1. In preparation for continuous operation, thyristor S_4 is turned on at t_0 as shown in Fig. 15. Thyristor S_4 will stay on until capacitor C_2 is charged from C_1 through D_2, L_3, and the injection bump magnets to a voltage $e_{C_2} \leq 2\,E_{C_1}$ at time t_1.

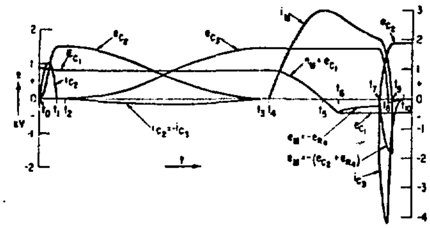

Fig. 15. Currents and voltages during first operation of the circuit of Figure 9.

2. At time t_2, thyristor S_5 is turned on. With $C_2 = C_3 = C$, the total energy stored in C_2 at time t_2 is transferred to C_3 at time t_3, except for losses, and S_5 turns off. The inductance L_2 never stores more than half the total energy during this transfer. The transfer current is

$$i_{C_3} = -i_{C_2} = \frac{E_{C_2}}{\omega_4 L}\,\varepsilon^{-\alpha_3 t}\,\sin\omega_4 t \qquad (17)$$

and the voltage on C_3 will be

$$e_{C_3} = \frac{E_{C_2}}{2}\left[1 - \varepsilon^{-\alpha_3 t}\left(\frac{\alpha_3}{\omega_4}\sin\omega_4 t + \cos\omega_4 t\right)\right], \quad (18)$$

where

$$\alpha_3 = R_{L_2}/2L_2\ ,$$

$$\omega_4 = \left(\frac{2}{L_2 C} - \alpha_3^{\,2}\right)^{1/2}\ ,$$

E_{C_2} = voltage on C_2 at t_2 ,

and

R_{L_2} = resistance of the C_2, L_2, L_3, C_3, and S_5 circuit.

3. The first magnet pulse is initiated at time t_4 by turning on S_3. As described previously, the current will rise, pass its peak at time t_5, and transfer into the crowbar. A negative voltage is trapped on C_1 at time t_6 by diode D_2 after the current has been transferred into the crowbar.

4. Injection is terminated at t_7 when S_6 and S_4 are turned on. This provides discharge paths for C_3 through L_4 via S_6 and through C_2 via S_6, S_3, S_4, and L_3. Saturable inductor L_3 keeps dI/dt within the ratings of S_6 and S_4 during the first few microseconds of the C_3 discharge. After ≤ 25 µs, S_3 has turned off. Thyristors S_6 will stay on until the current in L_4 has decayed to zero.

When S_3 turns off, the magnet discharges into C_2. The current and voltage follow the equations,

$$i_M = i_{C_2} = i_{M_{t_7}}\,\varepsilon^{-\alpha_4 t}\left(\cos\omega_5 t - \frac{\alpha_4}{\omega_5}\sin\omega_5 t\right)\ , \quad (19)$$

$$e_{C_2} = L_M i_{M_{t_7}} \left\{ \left[\alpha_4 - \epsilon^{-\alpha_4 t}(\alpha_4 \cos \omega_5 t - \omega_5 \sin \omega_5 t)\right] - \right.$$

$$\left. -\alpha_4 \left[1 - \epsilon^{-\alpha_4 t}\left(\cos \omega_5 t + \frac{\alpha_4}{\omega_5} \sin \omega_5 t\right)\right]\right\} , \qquad (20)$$

at time t_9 with $\omega t \approx \pi/2$ we have

$$e_{C_2} \approx \omega_5 L_M i_{M_{t_7}} \epsilon^{-\frac{\pi\alpha_4}{2\omega_5}} , \qquad (20')$$

where

$$\alpha_4 = (R_M + R_4)/2L_M ,$$

and

$$\omega_5 = \left(\frac{1}{L_M C_2} - \alpha_4^2\right)^{1/2} .$$

The value of C_2 has been chosen to resonate with the 60 μH magnet at 2 kHz in order to bring the current to zero in 125 μs. Diode D_3 switches water-cooled resistor R_5 in the turnoff circuit at time t_8 when the current in L_4 has passed its peak. Between times t_8 and t_{10}, the energy in L_4 dissipates mostly in R_5 and very little in the high-Q inductor.

This completes the first discharge cycle with capacitor C_1 having a negative charge and C_2 having a positive charge. The circuit is now ready to be charged from the dc power supply in preparation for the next magnet pulse.

Important features of the circuit as compared to the circuit of Fig. 3 are:

(a) The magnet voltage at turnoff is ≤ 1.5 kV.

(b) The coil windings of the magnets and chokes must only be rated for 1.5 kV.

(c) All thyristor and diode assemblies must only be rated for 1.5 kV.

(d) Capacitors C_2 and C_3 are rated for only 1.5 kV.

(e) The turnoff circuit carries a peak current of only 5.2 kA.

(f) The energy trapped in C_1 during discharge is used during the charge cycle. The energy recovered in C_2 from the magnet is used to charge C_3 and to terminate the next current pulse before it is dissipated in R_5.

(g) No separate turnoff power supply for charging C_3 is required.

Note that after S_3 has been turned off, the magnet voltage increases gradually and is small as compared to the 3.8 kV step change in the circuit of Fig. 3. This helps considerably to keep S_3 turned off. For example, operating with R_4 = 50 mΩ, we would have at the end of injection a magnet current i_M = 2 kA and a voltage $e_M \approx e_{R_4}$ = 100 V. After ≤ 25 μs required to turn off thyristor S_3, the potential on C_2 is, from Fig. 10, only about $e_{C_2} \approx$ 1500 V sin 18° = 460 V. In order to have at least that much potential across L_4, the initial voltage on C_3 must be, from Figure 8,

e_{C_3} > 460 V cos 54° = 783 V. For a magnet current of 2 kA, the circuit provides ∿1.3 kV on C_3.

The corresponding values, at the end of injection, when operating with R_4 = 150 mΩ are:

$$i_M = 1 \text{ kA}, \; e_M \approx e_{R_4} = 150 \text{ V},$$

$$e_{C_3} \approx e_{C_2} \approx \omega_5 L_M i_M \epsilon^{-\frac{\pi \alpha_4}{2 \omega_5}} = 674 \text{ V} ,$$

at turnoff, $e_{C2} \approx$ 674 V sin 18° = 208 V ,

and at turnoff, $e_{C3} \approx$ 674 V cos 54° = 396 V.

The above examples illustrate how the circuit changes the turnoff energy accumulated on C_2 automatically to match different values of magnet current. The current magnitude at the end of injection is determined by the injection time constant selected as shown by Eq. (14).

An oscilloscope picture of a typical magnet current pulse is shown in Fig. 16. At the end of the injection time, it can be noticed on the trace that the current decays for a very short time faster than described by Eq. (19). The reason for this is that, during the turnoff time of S_3, the magnet circuit is connected to C_3. This forces a rate of change of the magnet current

$$\frac{di_{t_3}}{dt} = \frac{e_{C_3} + e_{R_M} + e_{R_4}}{L_M} \qquad (21)$$

during the turnoff time.

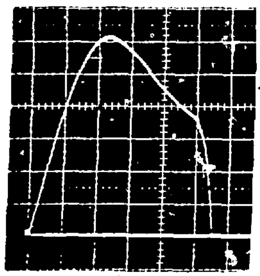

500 A / cm ↑

200 μs/cm →

Fig. 16. Oscilloscope picture of typical magnet current generated by the circuit of Fig. 9.

The sequence of operation for subsequent magnet pulses is as described for the first pulse, with one exception. With capacitor C_2 having a positive charge at the end of every magnet pulse, we no longer need to charge C_2 from capacitor C_1. Time-delay inductor L_3 is reset when the charge on C_2 is transferred to C_3.

<u>Circuit Components</u>

The circuit of Fig. 9 was built from parts available commercially or fabricated in our shop. A few details of special components are given below.

<u>Beam Bump Magnets.</u>

The magnets are of the picture-frame type and have cores assembled from 12-mil-thick silicon steel laminations. The magnet coils are wound with copper bus bars having cross sections of 1/8 x 1 in. Most of the external connections between the power supply and the magnets are made with flat-strip transmission lines; the rest are made with cables. On account of eddy-current losses, mainly in the magnet windings and magnet core laminations, the value of resistance R_M is larger than the copper resistance. In addition, the value of R_M changes during the pulse as di_M/dt varies. The effective circuit resistance is $\sim$ 62 mΩ during the rise time of the current and $\sim$ 16 mΩ when the magnets are crowbarred.

Thyristors and Diodes.

For clarity, the solid-state components of the circuit of Fig. 9 are shown as single units. In reality, this is only true for thyristors S_1 and S_2. All other components are made up by connecting two or more units in series. Voltage sharing between these units during steady-state and during transient conditions is achieved in the customary way with resistors and capacitors. The only thyristor assembly with stringent turnoff requirements is S_3. Here we use three matched thyristors in series, each having a reverse recovery charge of 36 ± 1 μC.

Turnoff Inductor L_4.

Inductor L_4 carries both the load current and the turnoff current pulse. The sum of these currents has a maximum value of 741 A rms with operating conditions as shown in Fig. 10. The turnoff circuit resonates at 5.9 kHz. At this frequency, the skin depth of copper is δ = 0.086 cm. For the inductor to have low losses, it was wound with 80 insulated wires of #14 AWG in parallel. This wire has a diameter d = 2 δ. The inductor has a C-core made from 12-mil laminations of grain oriented silicon steel with a cross section of 65 cm^2, an air gap of 4.2 cm and six turns.

Acknowledgements

It is a pleasure to acknowledge the support of Don McGhee, Don Reigle, and Gary Sprau. Don McGhee designed the logic circuits and the equipment layout; Don Reigle built the logic circuits; and Gary Sprau built most of the other components, assembled and wired the circuit, and tested it under the guidance of Don McGhee.